

[DOI]10.12016/j.issn.2096-1456.2024.01.007

· 临床研究 ·

基于 MobileNetV3 网络的龋病和根尖周炎根尖片的诊断

王凯欣¹, 刘丰¹, 曾令芳², 刘超³

1. 山东大学信息科学与工程学院, 山东 青岛(266237); 2. 济南市口腔医院儿童口腔1科, 山东 济南(250001);
3. 山东大学齐鲁医院口腔颌面外科, 山东 济南(250012)

【摘要】 目的 研究深度学习技术智能诊断龋齿和根尖周炎的效果, 初步探讨深度学习在口腔疾病诊断中的应用价值。方法 以2 298张包含健康牙齿、龋病、根尖周炎的根尖片数据集为研究对象, 随机划分为1 573张训练集图像, 233张验证集图像以及492张测试集图像。通过多种神经网络对比验证, 选择性能较好的 MobileNetV3 网络模型应用于牙病诊断, 并通过调整网络超参数优化模型。采用精确率、准确率、召回率和 F1 分数评估模型识别龋齿和根尖周炎的能力, 并使用类激活热力图对网络模型性能进行可视化分析。结果 基于 MobileNetV3 网络模型的牙齿病变检测算法对健康牙齿、龋病和根尖周炎进行分类的精确率、召回率和准确率分别为 99.42%、99.73% 和 99.60%, F1 分数为 99.57%, 达到了较为理想的智能诊断效果。可视化类激活热力图也显示出网络模型能够较为准确地提取牙科病变的特征。结论 基于 MobileNetV3 网络模型的牙齿病变检测算法能够排除图像质量和人为因素的干扰, 具有较高的诊断准确率, 可满足口腔医学教学和临床应用需求。

【关键词】 牙科病变; 龋病; 根尖周炎; 根尖片; 智能诊断; 图像处理; 深度学习; MobileNetV3 网络; 类激活图; 可视化分析

【中图分类号】 R78 **【文献标志码】** A **【文章编号】** 2096-1456(2024)01-0043-07

【引用著录格式】 王凯欣, 刘丰, 曾令芳, 等. 基于 MobileNetV3 网络的龋病和根尖周炎根尖片的诊断[J]. 口腔疾病防治, 2024, 32(1): 43-49. doi:10.12016/j.issn.2096-1456.2024.01.007.

MobileNetV3 network-based diagnosis of caries and periapical periodontitis from periapical films WANG Kaixin¹, LIU Feng¹, ZENG Lingfang², LIU Chao³. 1. School of Information Science and Technology, Shandong University, Qingdao 266237, China; 2. Pediatric Dentistry Department 1, Jinan Stomatological Hospital, Jinan 250001, China; 3. Department of Oral and Maxillofacial Surgery, Qilu Hospital of Shandong University, Jinan 250012, China
Corresponding author: ZENG Lingfang, Email: 2475973234@qq.com, Tel: 86-531-86261950; LIU Chao, Email: qiluliuchao@sdu.edu.cn, Tel: 86-18560083731

【Abstract】 Objective To research the effectiveness of deep learning techniques in intelligently diagnosing dental caries and periapical periodontitis and to explore the preliminary application value of deep learning in the diagnosis of oral diseases. **Methods** A dataset containing 2 298 periapical films, including healthy teeth, dental caries, and periapical periodontitis, was used for the study. The dataset was randomly divided into 1 573 training images, 233 validation images, and 492 test images. By comparing various neural network models, the MobileNetV3 network model with better performance was selected for dental disease diagnosis, and the model was optimized by tuning the network hyperparameters. The accuracy, precision, recall, and F1 score were used to evaluate the model's ability to recognize dental

【收稿日期】 2023-06-16; **【修回日期】** 2023-09-22

【基金项目】 国家自然科学基金面上项目(52172282)

【作者简介】 王凯欣, 硕士研究生, Email: 202232714@mail.sdu.edu.cn; 刘丰, 硕士研究生, Email: 15263667155@163.com, Tel: 86-18560083731

【通信作者】 曾令芳, 副主任医师, 硕士研究生, Email: 2475973234@qq.com, Tel: 86-531-86261950; 刘超, 副主任医师, 博士研究生, Email: qiluliuchao@sdu.edu.cn, Tel: 86-18560083731



微信公众号

caries and periapical periodontitis. Class activation map was used to visualization analyze the performance of the network model. **Results** The algorithm achieved a relatively ideal intelligent diagnostic effect with precision, recall, and accuracy of 99.42%, 99.73%, and 99.60%, respectively, and the F1 score was 99.57% for classifying healthy teeth, dental caries, and periapical periodontitis. The visualization of the class activation maps also showed that the network model can accurately extract features of dental diseases. **Conclusion** The tooth lesion detection algorithm based on the MobileNetV3 network model can eliminate interference from image quality and human factors and has high diagnostic accuracy, which can meet the needs of dental medicine teaching and clinical applications.

【Key words】 dental disease; caries; periapical periodontitis; periapical film; intelligent diagnosis; image processing; deep learning; MobileNetV3 network; class activation map; visualization analysis

J Prev Treat Stomatol Dis, 2024, 32(1): 43-49.

【Competing interests】 The authors declare no competing interests.

This study was supported by the grants from National Natural Science Foundation of China (No. 52172282).

牙科数字化X线成像是现代牙科领域中的一种重要技术,由于其操作方便、价格低廉、辐射较小,它广泛应用于诊断牙髓病、牙周病、牙齿缺损、根尖病变、牙槽骨吸收等情况^[1-2]。牙科数字化X线成像还可以帮助医生判断治疗方案的合理性以及评估治疗效果。但以往医生的诊断是通过肉眼观察,凭个人的经验进行分析,其诊断结论往往主观成分较多,尤其是上颌多个牙根有重叠现象时,其根分歧区域的牙槽骨显示不够直观。上颌乳牙根分歧出现病变时,由于此处乳牙牙根与恒牙胚有部分重叠,使骨质的吸收程度更加难以判断。近几年,深度学习在口腔医学临床研究中崭露头角^[3-6]。MobileNet系列网络具有检测速度快,检测效果好等优点^[7]。MobileNetV3网络是一种经典的轻量级神经网络,主要用于图像分类、目标识别和图像分割等任务^[8]。本研究拟探讨使用MobileNetV3在根尖片上进行病变分类诊断,为临床应用提供参考。

1 资料和方法

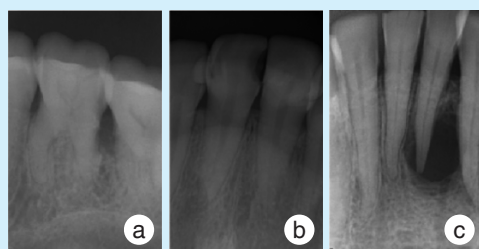
1.1 数据集建立

本研究数据为专业医师在临床诊断过程中拍摄的根尖片,所使用的图像采集设备为:Car-

estream Health口腔X射线机CS 2200和Sigma M数字化口内X射线成像系统M1。由专业医师诊断,将图像数据分为健康牙齿、龋病、根尖周炎3种类别,经三甲医院两名高级职称医师及一名中级职称医师分别独立标注,若出现标注不一致的情况,由专家们讨论确认。数据图像如图1所示。最终收集到2 298张研究数据,其中1 806张图像用于模型训练,包含1 573张训练集图像与233张验证集图像;测试数据包含492张图像,其中,正常牙齿图像113张,龋病图像136张,根尖周炎图像243张。训练集用于更新模型参数,调节模型权重;测试集评估模型效果与泛化能力。

1.2 MobileNetV3网络

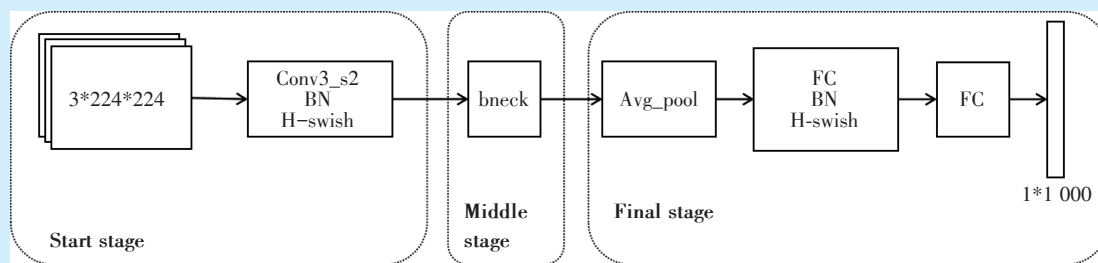
MobileNetV3是一种轻量化的分类模型,既保留了V1版本深度可分离卷积和V2版本的反残差线性瓶颈模块,保证了精度;又改进网络结构,减少了参数量^[9-10]。引入了注意力机制,包括SE(Squeeze-and-Excitation)模块。这样保留了高维特征空间,减少了反向传播的延迟,可以更加准确地对重要特征进行关注和增强^[11-12]。MobileNetV3网络结构可以分为3个阶段:起始阶段(Start stage),中间阶段(Middle stage)和最后阶段(Final stage),网络结构见图2。



a: a sample of a healthy tooth, its characteristics include a smooth tooth surface without visible cavities or periapical changes; b: a sample of dental caries, which is characterized by visible brown or black cavities on the tooth surface; c: a sample of periapical disease, showing a blurry and irregular dark area surrounding the root apex

Figure 1 Example of experimented data for MobileNetV3 network-based of caries and periapical periodontitis from periapical films diagnosis

图1 基于MobileNetV3网络的龋病及根尖周炎诊断实验数据实例



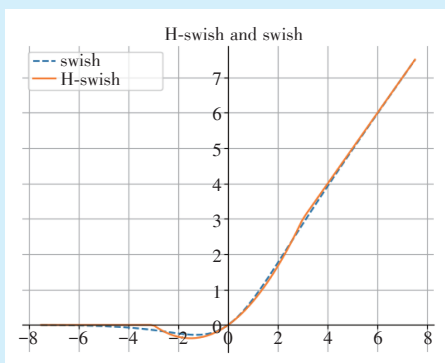
Start stage: including convolutional layer, batch normalization layer, and h-swish activation layer; middle stage: core module, mainly implementing channel separable convolution, SE attention mechanism, and residual connection; final stage: reduce computational complexity by advancing the average pooling layer; BN: batch normalization processing; FC: the abbreviation for fully connected layer

Figure 2 MobileNetV3 network structure diagram

图2 MobileNetV3网络结构示意图

1.2.1 起始阶段 更新了H-swish激活函数,相较于原始的swish激活函数,H-swish激活函数减少了计算量,降低了计算开销,并提高了速度^[13]。

H-swish激活函数计算公式:
$$H\text{-swish} = x \frac{\text{ReLU6}(x+3)}{6}$$
,特征图如图3所示。



The H-swish and Swish function curves are similar, retaining the smoothness advantage that plays an important role in optimization and generalization. Moreover, H-swish improves the inference speed of the network and is also very friendly to the quantization process

Figure 3 MobileNetV3 network activation function H-swish and original swish function

图3 MobileNetV3网络激活函数H-swish与原始swish函数

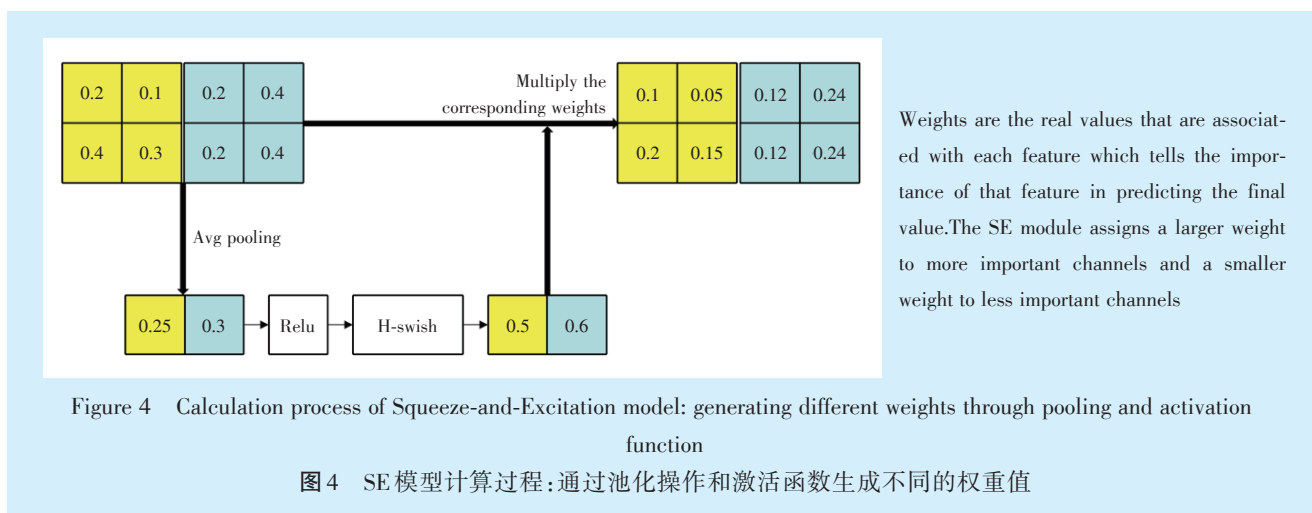
1.2.2 中间阶段 添加了SE注意力模型,用于提升精度。对于不同通道输入的特征矩阵,SE结构会通过池化操作和激活函数来生成不同的权重值,用于判断矩阵的重要程度。具体计算过程见图4。设通道数为2,SE模型会使用平均池化(average pooling)的方式提取特征均值,之后通过

Relu激活函数和H-swish激活函数计算出特征权重值,之后将权重值和原始矩阵相乘得到新的特征矩阵,结合特征通道来加强网络的学习能力^[14]。

1.2.3 最后阶段 将平均池化层提前,并通过一个卷积层修改通道数,拓展到更高维的空间。这样在预测阶段可以得到更丰富的特征来满足需求,并且在不造成精度损失的同时提升了计算速度,增强了网络性能。

1.3 模型优化

基于验证集初步评估模型能力并调整超参数,是模型训练的重要环节。合适的超参数可以优化特征表达,提升模型有效容量与参数实用性。而超参数调节不当则会影响优化,容易陷入局部最优解,造成过拟合等问题。为了保证实验结果准确,经过遍历性尝试,将网络的超参数调整至最优。通过超参数调整,本研究对于模型主要进行了以下几点优化:①将初始学习率优化为0.000 1,保证了模型容量和梯度更新的有效性^[15-16],防止网络迭代损失过大,导致无法收敛,落入局部最优解;②使用交叉熵作为网络损失函数,它的目标是 minimized 预测值与真实标签之间的差异,以使模型更准确地预测样本的类别,适用于多类别分类问题,可以避免在梯度下降时学习速率降低的问题,避免了梯度弥散,能更快地加速神经网络训练速度^[17-18];③选用Adam优化器来调节学习率的变化,对梯度的一阶矩估计和二阶矩估计进行综合考虑,计算出更新步长,对内存需求较小且可以自适应学习率,使得网络收敛更加平稳,提高计算效率,降低计算开销;④对其他超参数进行了遍历性调整,将网络效能发挥至最优^[19]。其中, Batch_size代表输入网络的批次大小,将其设置为



32, 利用较大的 Batch_size 可以提高内存利用率和矩阵乘法的并行效率; Epochs 代表迭代次数, 设置为 100, 保证网络收敛至稳定。

1.4 评价指标

分类算法的评价指标包含很多种, 本研究使用精确率 (precision, P)、召回率 (recall, R)、准确率 (accuracy, A) 以及 F1 分数 (F1 score, F1) 作为衡量指标。

精确率用于衡量网络模型对于正样本的检测准确程度, 表示为所有被检测为正样本的数量中, 实际正样本所占的概率。精确率越高, 误报率越小。该计算指标的计算公式: $P = \frac{TP}{TP+FP}$, 式中, TP 表示真阳性样本, FP 代表假阳性样本。

召回率用于衡量网络模型的查全率, 表示为在实际为正样本的总体中被检测为正样本的概率。召回率越高, 漏报率越小。计算公式为: $R = \frac{TP}{TP+FN}$,

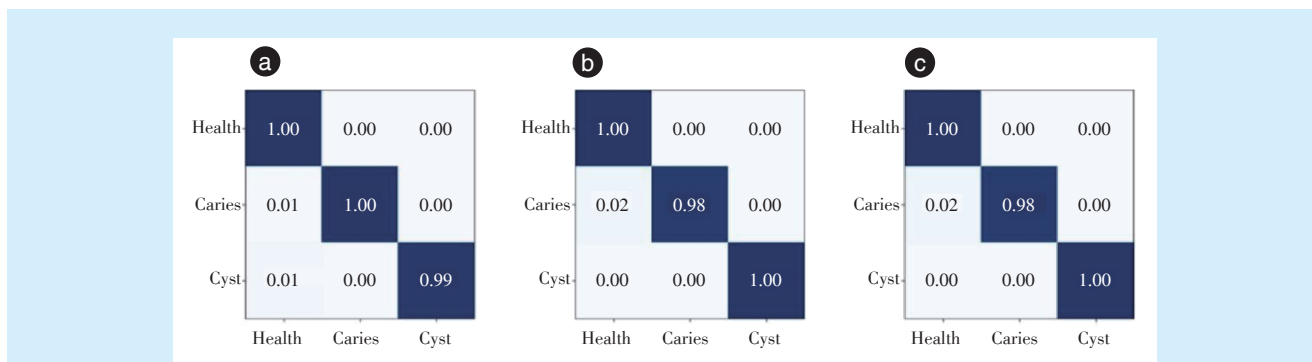
式中, TP 表示正阳性样本, FN 代表假阴性样本。

准确率用于衡量网络模型对于所有样本的检测准确程度, 表示为检测的所有样本中, 检测正确的样本概率。准确率越高, 网络检测越可信, 计算公式: $A = \frac{TP+TN}{TP+FP+TN+FN}$ 。F1 分数则被定义为精确率和召回率的调和平均数, 综合了两者的产出结果, 计算公式: $F1\ score = \frac{2 \times P \times R}{P+R} = \frac{2TP}{2TP+FP+FN}$, 式中, TP 表示真阳性样本, FP 代表假阳性样本, TN 表示真阴性样本, FN 代表假阴性样本, P 表示精确率, R 表示召回率。

2 结果

2.1 结果对比

本研究测试算法与现有研究的分类算法在创建的数据集上进行训练和测试, 本文网络测试结果与其它模型对比的混淆矩阵如图 5 所示。



a: MobileNetV3 network; b: EfficientNetV2 network; c: DensNet-121 network. The confusion matrix represents each column as the predicted class and each row as the true class of the data. The elements in the matrix represent the prediction probabilities. The closer the diagonal element is to 1, the better the classification effect

Figure 5 Confusion matrix of MobileNetV3 model and other models

图5 MobileNetV3 模型及其他模型混淆矩阵

通过图5计算可得,最终本文算法精确率、召回率和准确率分别为99.42%、99.73%和99.60%,表明本文算法拥有相对较高的检测准确性,并且漏报和误报的情况也相对较少;F1分数为99.57%,拥有相对最好的网络性能。表1为实验结果和其它网络模型的对比结果。表中各计算结果取3个种类的平均值,结果保留两位小数。

表1 MobileNetV3模型与其他模型测试结果

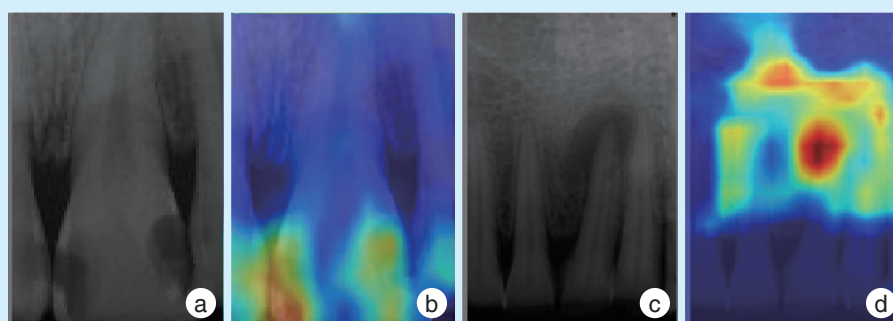
Table 1 Test results of MobileNetV3 model and other models

Network name	Precision (%)	Recall (%)	Accuracy (%)	F1 score
MobileNetV3	99.42	99.73	99.60	99.57
EfficientNetV2	99.42	98.53	99.60	98.97
DensNet-121	97.41	97.79	99.39	97.60

2.2 热力图可视化

为验证分类结果准确性,使用类激活热力图(class activation map, CAM)作为可视化工具,直观

显示图像中各部分对于MobileNetV3网络的最终决策影响程度,作为一种定性评价方式,增强模型行为的认知和性能的评估^[20]。类激活热力图是与特定输出类别相关的二维分数网格,对任何输入图像的每个位置都要进行计算,它表示每个位置对该类别的重要程度。热力图中重要程度会被以颜色的形式显示,输入数据越重要的区域,颜色越接近红色(暖色),表明该部分对于网络识别该数据的贡献越大;反之重要程度越低,颜色越接近蓝色(冷色),表明贡献越小。对分类结果进行热力图可视化,图6a & 6b为龋病原图像与类激活热力图对比,图6c & 6d为根尖周炎原图与热力图对比。观察图像可得,龋病图像红色区域集中于牙冠部分,根尖周炎图像红色区域则集中与根尖病变部分,表明网络模型经过训练,能够较为准确地学习并识别龋病与根尖周炎的特征,并将注意力更多地集中在病变区域。



a: X-ray image of dental caries; b: class activation map of dental caries; c: X-ray image of periapical lesions; d: class activation map of periapical lesions. The dental crown is identified as an important region related to dental caries by the neural network, while the area of root apex pathology is identified as an important region related to periapical lesions. The closer the color is to red, the greater the contribution of this part to the network's recognition of the data, the closer the color is to blue, the smaller the contribution

Figure 6 Display of class activation map

图6 类激活热力图展示

3 讨论

随着医疗领域智能化和数字化诊断的发展,数据量越来越庞大,检测指标要求精度也在不断上涨,这促使了具有强大数据处理能力的深度学习网络与医疗领域的融合。一种口腔疾病智能诊断的工具可以辅助医师诊断,提高诊疗效率^[21-23]。Zhang等^[24]基于卷积神经网络实现了牙齿X线片图像分割,提高了牙病诊断准确率。Megalani等^[25]利用混合神经网络(hybrid neural network, HNN)实现龋齿影像分类,在龋齿检测中具有一定的价值。Ghaznavi等^[26]利用AlexNet网络对下颌曲面体层片进行牙齿状态的识别,提出了确定颌骨位置

并达到牙齿诊断的智能方法。Liu等^[27]提出利用DensNet-121网络实现对于龋齿和根尖周病变的诊断,得到了较高的诊断准确率,该研究组提出使用YOLOv5网络实现对X线片的病变位置的精确定位,最终准确率达到95%。本研究提出使用MobileNetV3算法进行根尖片的病变检测,将医院收集的根尖片作为实验数据,由专业医师按照不同病变种类对数据进行分类,在数据集上进行训练、测试,并调整了网络超参数,得到效果较好的网络模型,并从准确率、精确率、召回率和F1分数4个不同的角度评估网络模型。最终经过测试,算法模型在根尖片上可以实现病变诊断,准确率达到

99.60%, 尤其对于多个组织重叠处肉眼不易判断的病变, 有极大的优势。而且对于提高治疗的精准度和效率, 以及缓解我国口腔医疗资源紧张的局面具有潜在价值。

目前, 有大量基于深度学习的龋病和根尖周病辅助诊断模型研究^[28-30]。Lee等^[31]提出了一种基于根尖片的深度学习算法以自动诊断龋病, 对前磨牙及磨牙龋病诊断的准确率分别达到89%和88%; Zhu等^[32]利用Faster-RCNN基于根尖片预测龋齿病变的数量和位置, 像素准确率和F1分数分别达到73.49%和68%; Orhan等^[33]对根尖周病CBCT影像进行自动诊断, 其可靠性为92.8%。与其他研究相比, 本研究同时诊断龋病与根尖周炎, 利用轻量化分类模型达到了更高的诊断准确率。

以上结果表明, 本研究使用的方法在根尖片病变的分类诊断任务上具有较高的识别准确率, 能够初步应用于龋病及根尖周炎的诊断, 有望进一步大样本验证后逐步推广于临床诊断。但本研究模型依然存在一定局限性。第一, 本研究数据集具有一定局限性, 数据来源较为单一, 虽然在本数据集上取得了较高的诊断精度, 但是泛化能力有待进一步提升, 后续将引入更多病例和更丰富的数据集, 从不同机构或多个中心大规模收集数据, 以进一步增强模型的泛化能力; 第二, 由于本研究处于初期阶段, 模型有待临床验证, 在之后的研究中将不断对算法进行优化与调整, 进一步提升模型可信度、通用性与安全性; 第三, 当前主要对根尖周炎进行分析, 后续考虑对根尖周病的其他几种类型(如致密性骨炎、牙骨质增生、牙骨质骨结构不良等)进行诊断, 并结合口腔影像数据和其他临床信息(如病历等)进行跨模态学习, 在诊断疾病的同时给予参考诊疗方案。

【Author contributions】 Wang KX processed the research and wrote the article. Liu F and Zeng LF processed the research and revised the article. Liu C designed the study and revised the article. All authors read and approved the final manuscript as submitted.

参考文献

- [1] Hart D, Hillier MC, Wall BF. National reference doses for common radiographic, fluoroscopic and dental X-ray examinations in the UK [J]. *Br J Radiol*, 2009, 82(973): 1-12. doi: 10.1259/bjr/12568539.
- [2] Rad AE, Rahim MS, Rehman A, et al. Digital dental X-ray database for caries screening [J]. *3D Res*, 2016, 7(2):18. doi: 10.1007/s13319-016-0096-5.
- [3] Sun ML, Liu Y, Liu G, et al. Application of machine learning to stomatology: a comprehensive review [J]. *IEEE Access*, 2020, 8: 184360-184374. doi: 10.1109/ACCESS.2020.3028600.
- [4] Mohammad-Rahimi H, Motamedian SR, Pirayesh Z, et al. Deep learning in periodontology and oral implantology: a scoping review [J]. *J Periodontol Res*, 2022, 57(5): 942-951. doi: 10.1111/jre.13037.
- [5] Chu CS, Lee NP, Ho JWK, et al. Deep learning for clinical image analyses in oral squamous cell carcinoma: a review [J]. *JAMA Otolaryngol Head Neck Surg*, 2021, 147(10): 893-900. doi: 10.1001/jamaoto.2021.2028.
- [6] Sukegawa S, Tanaka F, Nakano K, et al. Effective deep learning for oral exfoliative cytology classification [J]. *Sci Rep*, 2022, 12: 13281. doi: 10.1038/s41598-022-17602-4.
- [7] Edel G, Kapustin V. Exploring of the MobileNet V1 and MobileNet V2 models on NVIDIA Jetson Nano microcomputer [J]. *J Phys: Conf Ser*, 2022, 2291(1): 012008. doi: 10.1088/1742-6596/2291/1/012008.
- [8] Deng T, Wu Y. Simultaneous vehicle and lane detection via MobileNetV3 in car following scene [J]. *PLoS One*, 2022, 17(3): e0264551. doi: 10.1371/journal.pone.0264551.
- [9] Zhang Z, Yang X, Luo N, et al. A novel method for Pu-erh tea face traceability identification based on improved MobileNetV3 and triplet loss [J]. *Sci Rep*, 2023, 13(1): 6986. doi: 10.1038/s41598-023-34190-z.
- [10] Altun M, Gürüler H, Özkaraca O, et al. Monkeypox detection using CNN with transfer learning [J]. *Sensors*, 2023, 23(4): 1783. doi: 10.3390/s23041783.
- [11] Guo MH, Xu TX, Liu JJ, et al. Attention mechanisms in computer vision: a survey [J]. *Comp Visual Media*, 2022, 8(3): 331-368. doi: 10.1007/s41095-022-0271-y.
- [12] Wang J, Luan Z, Yu Z, et al. Superpixel segmentation with squeeze-and-excitation networks [J]. *SIViP*, 2022, 16(5): 1161-1168. doi: 10.1007/s11760-021-02066-2.
- [13] Li Y, Chai Y, Yin H, et al. A novel feature learning framework for high-dimensional data classification [J]. *Int J Mach Learn Cybern*, 2021, 12(2): 555-569. doi: 10.1007/s13042-020-01188-2.
- [14] Allu R, Padmanabhuni VNR. Predicting the success rate of a start-up using LSTM with a swish activation function [J]. *J Contr Decis*, 2022, 9(3): 355-363. doi: 10.1080/23307706.2021.1982781.
- [15] Yang L, Shami A. On hyperparameter optimization of machine learning algorithms: theory and practice [J]. *Neurocomputing*, 2020, 415(20): 295-316. doi: 10.1016/j.neucom.2020.07.061.
- [16] Ansbacher-Feldman Z, Syngelaki A, Meiri H, et al. Machine-learning-based prediction of pre-eclampsia using first-trimester maternal characteristics and biomarkers [J]. *Ultrasound Obstet Gynecol*, 2022, 60(6): 739-745. doi: 10.1002/uog.26105.
- [17] Li L, Doroslovački M, Loew MH. Approximating the gradient of cross-entropy loss function [J]. *IEEE Access*, 2020, 8: 111626-111635. doi: 10.1109/ACCESS.2020.3001531.
- [18] Malhotra P, Gupta S, Koundal D, et al. Deep neural networks for medical image segmentation [J]. *J Healthc Eng*, 2022, 2022: 9580991. doi: 10.1155/2022/9580991.

- [19] Murugesan B, Liu B, Galdran A, et al. Calibrating segmentation networks with margin-based label smoothing [J]. *Med Image Anal*, 2023, 87: 102826. doi: 10.1016/j.media.2023.102826.
- [20] Shin H, Ahn Y, Song M, et al. Visualization for explanation of deep learning-based defect detection model using class activation map [J]. *Comput Mater Continua*, 2023, 75(3): 4753-4766. doi: 10.32604/cmc.2023.038362.
- [21] Luo D, Zeng W, Chen J, et al. Deep learning for automatic image segmentation in stomatology and its clinical application [J]. *Front Med Technol*, 2021, 3: 767836. doi: 10.3389/fmedt.2021.767836.
- [22] Mohammad - Rahimi H, Rokhshad R, Bencharit S, et al. Deep learning: a primer for dentists and dental researchers [J]. *J Dent*, 2023, 130: 104430. doi: 10.1016/j.jdent.2023.104430.
- [23] Sivari E, Senirkentli GB, Bostanci E, et al. Deep learning in diagnosis of dental anomalies and diseases: a systematic review [J]. *Diagnostics (Basel)*, 2023, 13(15): 2512. doi: 10.3390/diagnostics13152512.
- [24] Zhang C, Wilson M. Research on dental disease recognition based on convolutional neural network [J]. *J Med Imaging Hlth Inform*, 2020, 10(8): 1938-1942. doi: 10.1166/jmihi.2020.3098.
- [25] Megalan LL, Kalapalatha RT. Learning compact and discriminative hybrid neural network for dental caries classification [J]. *Microprocess Microsyst*, 2021, 82: 103836. doi: 10.1016/j.micpro.2021.103836.
- [26] Ghaznavi Bidgoli SA, Sharifi A, Manthouri M. Automatic diagnosis of dental diseases using convolutional neural network and panoramic radiographic images [J]. *Comput Meth Biomech Biomed Eng*, 2021, 9(5): 447-455. doi: 10.1080/21681163.2020.1847200.
- [27] Liu F, Gao L, Wan J, et al. Recognition of digital dental X-ray images using a convolutional neural network [J]. *J Digit Imaging*, 2023, 36(1): 73-79. doi: 10.1007/s10278-022-00694-9.
- [28] Li S, Liu J, Zhou Z, et al. Artificial intelligence for caries and periapical periodontitis detection[J]. *J Dent*, 2022, 122: 104107. doi: 10.1016/j.jdent.2022.104107.
- [29] Bui TH, Hamamoto K, Paing MP. Automated caries screening using ensemble deep learning on panoramic radiographs[J]. *Entropy (Basel)*, 2022, 24(10): 1358. doi: 10.3390/e24101358.
- [30] Oztekin F, Katar O, Sadak F, et al. An explainable deep learning model to prediction dental caries using panoramic radiograph images[J]. *Diagnostics*, 2023, 13(2): 226. doi: 10.3390/diagnostics13020226.
- [31] Lee JH, Kim DH, Jeong SN, et al. Detection and diagnosis of dental caries using a deep learning-based convolutional neural network algorithm [J]. *J Dent*, 2018, 77: 106-111. doi: 10.1016/j.jdent.2018.07.015.
- [32] Zhu Y, Xu T, Peng L, et al. Faster-RCNN based intelligent detection and localization of dental caries [J]. *Displays*, 2022, 74: 102201. doi: 10.1016/j.displa.2022.102201.
- [33] Orhan K, Bayrakdar IS, Ezhov M, et al. Evaluation of artificial intelligence for detecting periapical pathosis on cone-beam computed tomography scans [J]. *Int Endod J*, 2020, 53(5): 680-689. doi: 10.1111/iej.13265.

(编辑 周春华,曾雄群)



Open Access

This article is licensed under a Creative Commons Attribution 4.0 International License.

Copyright © 2024 by Editorial Department of Journal of Prevention and Treatment for Stomatological Diseases



官网